



Acetylcholine biosensor based on the electrochemical functionalization of graphene field-effect transistors

Gonzalo E. Fenoy^{a,b}, Waldemar A. Marmisollé^a, Omar Azzaroni^{a,c,*}, Wolfgang Knoll^{d,e}

^a Instituto de Investigaciones Físicoquímicas Teóricas y Aplicadas (INIFTA), Departamento de Química, Facultad de Ciencias Exactas, Universidad Nacional de La Plata (UNLP), CONICET, Diagonal 113 and 64, La Plata, 1900, Argentina

^b Instituto de Investigación e Ingeniería Ambiental, Universidad Nacional de San Martín, 25 de Mayo y Francia, 1 Piso, 1650, Buenos Aires, Argentina

^c CEST-UNLP Partner Lab for Bioelectronics, Diagonal 64 y 113, La Plata, 1900, Argentina

^d CEST - Competence Center for Electrochemical Surface Technologies, Konrad Lorenz Strasse 24, 3430, Tulln, Austria

^e Austrian Institute of Technology, Donau-City-Strasse 1, 1220, Vienna, Austria

ARTICLE INFO

Keywords:

Graphene
Field-effect transistor
Acetylcholine
Acetylcholinesterase
gFETs
Electropolymerization

ABSTRACT

We present a new strategy of Acetylcholinesterase (AChE) immobilization on graphene field-effect transistors (gFETs) for building up Acetylcholine sensors. This method is based on the electrosynthesis of an amino moiety-bearing polymer layer on the graphene channel. The film of the copolymer poly(3-amino-benzylamine-co-aniline) (PABA) does not only provide the suitable electrostatic charge and non-denaturing environment for enzyme immobilization, but it also improves the pH sensitivity of the gFETs (from 40.8 to 56.3 $\mu\text{A}/\text{pH}$ unit), probably due to its wider effective pKa distribution. The local pH changes caused by the enzyme-catalyzed hydrolysis produce a shift in the Dirac point of the gFETs to more negative values, which are evidenced as differences in the gFET conductivity and thereby constituted the signal transduction mechanism of the modified transistors. In this way, the constructed biosensors showed a LOD of 2.3 μM and were able to monitor Ach in the range from 5 to 1000 μM in a flow configuration. Moreover, they showed a sensitivity of $-26.6 \pm 0.7 \mu\text{A}/\text{Ach}$ decade and also exhibited a very low RSD of 2.6%, revealing good device-to-device reproducibility. The biosensors revealed an excellent selectivity to interferences known to be present in the extracellular milieu, and the response to Ach was recovered by 97.5% after the whole set of interferences injected. Finally, the biosensors showed a fast response time, with an average value of 130 s and a good long-term response.

1. Introduction

Acetylcholine (ACh) was the first identified neurotransmitter and is recognized to play a crucial role in the cholinergic system as a transmitter of impulses on the cholinergic synapse (Sattarahmady et al., 2010). Moreover, the alteration of central cholinergic transmission is coupled to a number of brain disorders including Alzheimer's disease, Parkinson's disease, addiction, epilepsy, schizophrenia, and depression (Kong et al., 2019). In a recent report by the World Health Organization, it was stated that neurological disorders are affecting nearly 1 in 100 of the world's inhabitants (Kergoat et al., 2014; World Health Organization, 2006). Since abnormal levels of acetylcholine are related to such disorders (Mitchell, 2004), considerable effort has been devoted in recent years to develop highly sensitive and specific techniques to detect

the local Ach concentration.

Although different analytical procedures exist for Ach detection, including capillary electrophoresis and liquid chromatography, they are usually expensive and time-consuming (Andreescu and Marty, 2006; Sangubotla and Kim, 2018). Therefore, it is a priority to develop a portable and rapid detection strategy for Ach. Here is where Field-Effect Transistors (FETs) technology emerges as a highly sensitive option for biosensing, which also allows for miniaturization. Particularly, graphene-based field effect transistors (gFETs) have gained much attention in last years because they are suitable for real-time, high-throughput and highly sensitive detection (Andronescu and Schuhmann, 2017). The sensing principle of gFETs roots on a change of the electrical conductance of the graphene channel upon adsorption of ions or molecules on the sensor surface. In this way, as pH changes are able to modify

* Corresponding author. Instituto de Investigaciones Físicoquímicas Teóricas y Aplicadas (INIFTA), Departamento de Química, Facultad de Ciencias Exactas, Universidad Nacional de La Plata (UNLP), CONICET, Diagonal 113 and 64, La Plata, 1900, Argentina.

E-mail address: azzaroni@inifta.unlp.edu.ar (O. Azzaroni).

URL: <https://softmatter.quimica.unlp.edu.ar> (O. Azzaroni).

<https://doi.org/10.1016/j.bios.2019.111796>

Received 21 September 2019; Received in revised form 17 October 2019; Accepted 17 October 2019

Available online 22 October 2019

0956-5663/© 2019 Elsevier B.V. All rights reserved.

the doping of graphene, gFETs can also work as pH sensors (Fu et al., 2017). If the pH variation is generated by an enzymatic reaction, one could build a biosensor by immobilizing an enzyme close to the graphene surface and detect changes in the analyte concentration by the conductivity change induced by the local pH change, this constituting the signal transduction mechanism of the biosensor. Recently, this approach has been successfully applied to the determination of relevant biomolecules, such as urea (Piccinini et al., 2017), acetylcholine (Chae et al., 2018), and L-arginine (Berninger et al., 2018).

Nevertheless, as the performance of the biosensor greatly depends on the properties of the interfacial architecture, the enzyme must be immobilized in a way that guarantees the conservation of its biological activity and the accessibility to its active sites, as well as the functionality of the transducing element (Bliem et al., 2018). To date, the majority of the research efforts in graphene-based FETs biosensors have focused on the immobilization of enzymes by covalent binding to functional groups of previously modified graphene or to a linker molecule (Fu et al., 2017). This is the case of all reports on gFETs for Ach sensing (Chae et al., 2018; Hess et al., 2014; Sohn et al., 2013). However, the covalent attachment of biomolecules presents some drawbacks, such as poor reproducibility and, as crucial groups can be involved in the immobilization, the possibility of disrupting the folding and functionality of the enzyme, thus affecting the biosensor performance (Sheldon and van Pelt, 2013; Vakurov et al., 2005). Moreover, direct covalent attachment to the graphene surface can also provoke damage to the sp^2 structure of the graphene and therefore deteriorate the signal transduction (Bliem et al., 2018; Niyogi et al., 2010).

Polyelectrolyte adsorption on gFETs constitutes a versatile and simple technique of functionalization that can provide adequate moieties for subsequent electrostatic enzyme immobilization, preserving the bioactive functionality of the enzyme and ensuring substrate accessibility (Chakrabarti et al., 2013). Within this scenario, amino-moieties bearing polymers have been recently reported to improve the pH response of gFETs, as the change in the degree of protonation of polymers in the vicinity of the graphene induces a shift in the Fermi level (Hess et al., 2014; Piccinini et al., 2017).

On the other hand, electropolymerization offers several advantages as functionalization method, such as a precise control on the polymer film thickness and mechanical stability towards detachment. In the typical modification by polyelectrolytes adsorption, no real control on the amount of polymer deposited is attained as it usually takes place until surface saturation. Moreover, in opposition to the typical layer-by-layer fabrication technique, a counter-polyelectrolyte is not required, producing nanofilms with chemical homogeneity. Although the electrochemical functionalization of graphene has been already reported (Chakrabarti et al., 2013) and even the non-covalent electrochemical attachment of aromatic amino groups on gFETs was studied in order to modify the Dirac voltage of the transistors (Zuccaro et al., 2015), as far as we know, there have been no reports on the electrochemical functionalization of gFETs with polymers for biosensing applications.

Among electroactive polymers, polyaniline (Pani) and related polymers have been much employed in a variety of applications. However, the electrosynthesis of polymers with pendant primary amine groups is not trivial. In this sense, we have recently developed a synthetic procedure that allows obtaining stable and electroactive films of poly(3-amino-benzylamine-co-aniline) (PABA) with a considerable proportion of primary amine groups by electropolymerization (Marmisollé et al., 2015). Within the field of gFETs, the presence of a variety of amine-imine groups in PABA (those from the Pani-like backbone and those from the pendant groups) could be able to transduce pH changes into different sensor responses in a wide pH range. Therefore, in this work we explored the electrodeposition of PABA on gFETs as an alternative for the construction of neurotransmitter biosensors. Thus, we developed a new strategy for building up Ach biosensors by immobilizing AchE on gFETs previously functionalized by PABA electrosynthesis (AchE-PABA-gFETs) (Scheme 1). The PABA film does not only

provide the suitable environment for enzyme immobilization, but it also improves the pH sensitivity of the gFETs. In this way, the local pH changes caused by the enzyme-catalyzed hydrolysis produce differences in the gFET conductivity, which were employed as the signal transduction mechanism to sense Ach in a flow configuration.

2. Results and discussion

2.1. gFETs preparation, characterization and performance

The gFETs were fabricated using a wet chemical approach on interdigitated electrodes (IDEs) (see SI). Briefly, the glass space between the Au IDEs was modified with APTES and, in the next step, the introduced amino groups were used for anchoring the negatively charged GO sheets by drop-casting. Next, two reduction steps were performed (Fig. S1).

An electrolyte-gated configuration (Fig. 1A) was used for the gFETs measurements. By changing the voltage of the gate electrode (V_G) at a constant drain-source voltage (V_{DS}), it is possible to modulate the conductivity of the rGO channel, resulting in a V-shaped transfer curve. The point of the minimum conductivity is called Dirac point and occurs at the Dirac voltage (V_i). Voltages more negative than V_i imply majority of holes as charge carriers, whereas carriers are electrons for more positive voltages. Charge carrier mobility for the present gFETs was determined to be $12 \text{ cm}^2 \text{ V}^{-1} \text{ s}^{-1}$ (see SI).

The inset in Fig. 1B shows a commercial IDE, whereas the SEM image in Fig. 1C (see also Fig. S2) clearly reveals the effective coverage and bridging of the electrodes by rGO. The slight variation introduced to the protocol reported before (Piccinini et al., 2017) resulted in very high device transconductance values (up to $1600 \mu\text{S}$, Fig. S3B), stated as a critical requirement for the development of highly sensitive biosensors (Zhang et al., 2015). Moreover, the use of IDE allows for a stable response as well as high device-to-device reproducibility (the RSD of conductivity values for the finished gFETs was less than 15% for 20 transistors).

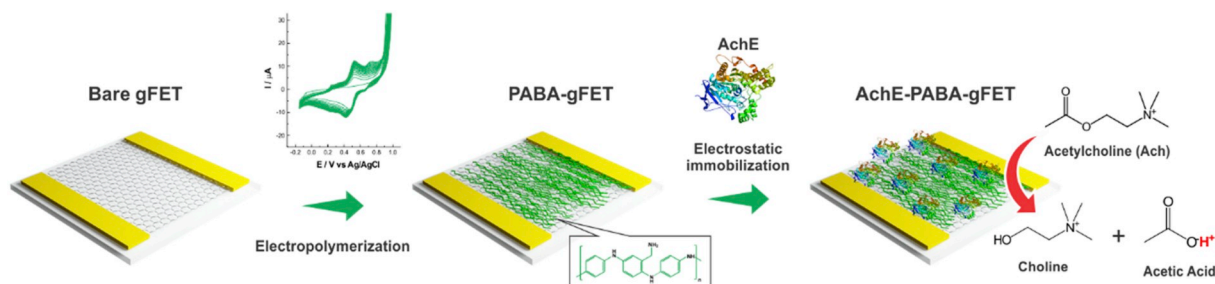
Scheme 1 shows the successive steps for the construction of biosensors and the enzyme-catalyzed hydrolysis which constitutes the signal transduction mechanism.

2.2. PABA electropolymerization and pH response improvement

In order to turn the gFETs into an adequate platform to immobilize AchE, the electropolymerization of PABA in acidic medium was performed as described in previous works (Fenoy et al., 2018b) (see SI for details). The electrosynthesized copolymer bears pendant amino groups that allow for the incorporation of different molecules and functionalities. The complete coverage and the good electronic conductivity of rGO between and onto the Au pads has been confirmed in previous works by using different techniques as SECM and KFM (Kotłowski et al., 2018; Reiner-Rozman et al., 2015), which ensures a suitable surface for electropolymerization.

Voltammograms of the PABA electrodeposition are shown in Fig. 2A. The features of the voltammetric response are very similar to those reported on gold electrodes (Fenoy et al., 2018a; Marmisollé et al., 2015), even when comparing the current density values during the electropolymerization. From EQCM results, a film thickness of approximately 7 nm can be estimated for the PABA-modified gFETs (Fenoy et al., 2018b). The effective deposition of the copolymer can be observed by SEM (Fig. 2B).

The transfer characteristics at pH 7 of a gFET before and after the polymer electrodeposition are shown in Fig. 2C. After the electropolymerization, there is a shift of 50 mV in the Dirac point to more negative values. This behavior has been attributed to the electrostatic gating effect of the positively charged copolymer onto the transistors (Wang and Burke, 2014). The deposition of cationic polyelectrolytes and polymer brushes have been reported to cause the same effect in graphene field-effect transistors (Hess et al., 2014; Piccinini et al., 2017).



Scheme 1. Representation of the different functionalization steps of the gFETs for the fabrication of Ach biosensors and the AchE-catalyzed hydrolysis of acetylcholine.

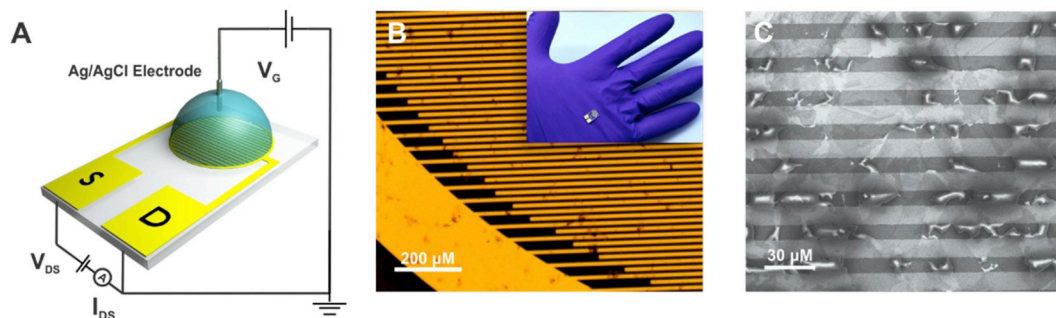


Fig. 1. Schematic illustration of the electrolyte-gated configuration (A). Optical micrograph of a gFET and picture of the commercial IDE (inset) (B). SEM image of the rGO-modified IDE (C).

Furthermore, the PABA-gFETs transfer characteristics and the transconductance curve at pH 7 (KCl 10 mM, HEPES 0.1 mM) are shown in Fig. S4. The transconductance values remains barely the same for the gFETs before (Section 3.1, Fig. S3) and after the electropolymerization (which has been reported as a decisive parameter for highly sensitive sensors), revealing that no worsening of the gFETs performance occurs after the polymer deposition.

As the signal transduction mechanism of our devices is based on the detection of pH changes caused by the enzyme-catalyzed hydrolysis, the pH response of the bare (Fig. S3A) and PABA-gFETs was studied in both static and flow conditions (Fig. 2D and E). As the pH decreases, the Dirac point of the gFETs shifts to more negative values due to H_3O^+ adsorption (n-type doping). Similarly, at basic pH, the OH^- adsorption (p-type doping) shifts the Dirac point to more positive voltage values (Salvo et al., 2018). For a real-time measurement (continuous flow mode, operational setup for potential biosensors), the gate potential is fixed at a value at which no chemical reaction is known to occur ($V_G = -0.2$ V in this case). As the gFET is biased in the hole regime (V_G lower than the Dirac point), lowering the solution pH yields a higher drain-source current (at a fixed positive V_{DS}). In this continuous flow configuration, the pH sensitivity of the bare gFET system was 40.8 ± 1.0 $\mu\text{A}/\text{pH}$ unit. Interestingly, the electrodeposited polymer was found to improve the pH sensitivity at this fixed gate potential by 38% (from 40.8 to 56.3 $\mu\text{A}/\text{pH}$ unit) (Fig. 2D). This phenomenon was already reported for PEI and cationic polymer brush-modified gFETs, and it was postulated that the change in the degree of protonation of polymers induces a shift in the graphene Fermi level and affects the pH response of the transistors (Hess et al., 2014; Piccinini et al., 2017). In those works, the rGO/graphene channel surface was modified with polymers having a pK_a around 8 (8–9 for PEI and around 8 for N,N-dimethylaminoethyl methacrylate brushes). In case of PABA, the composition of the copolymer has been determined to be about 30% molar of ABA (Marmisollé et al., 2015), so it is necessary to take into account the differences between aniline and 3-aminoethylamine residues for the analysis of the protonation states. In the case of the polyaniline, pK_a are reported to be between 2.5 (assigned to $-\text{NH}_2^-$) and 5.5 ($-\text{NH}^+ =$ species) (Marmisollé et al., 2014;

Ray et al., 1989). For polyaminobenzylamines, the pendant amino groups are still protonated at neutral pH (Marmisollé et al., 2015; Raffa et al., 2006; Zuccaro et al., 2015). The multiple protonation states of the electrodeposited copolymer may be ascribed to be the reason for the improved pH response of the PABA-gFETs compared to that of PEI-modified ones (38% vs 28%). The same argument has been ascribed for improvement of the pH response at basic pH values and the lower pH sensitivity in acidic conditions in the case of the brush-modified gFETs. In summary, the electrodeposited co-polymer does not only act as a priming layer for the enzyme anchoring, but it also improves the pH sensitivity of the device.

2.3. Acetylcholinesterase immobilization

The immobilization of enzymes is one of the most important steps in enzyme-based biosensor design and development as it affects sensitivity, stability, response time and reproducibility. Particularly, the anchoring of AchE was studied extensively along the last years (Andreescu and Marty, 2006; Diao et al., 2018). Among the existing methods, electrostatic immobilization can surpass some of the drawbacks of ordinary covalent attachment, such as poor reproducibility and the possibility of disrupting the folding and functionality of the enzyme, as crucial groups can be involved in the immobilization (Sheldon and van Pelt, 2013; Vakurov et al., 2005). Moreover, direct covalent attachment to the graphene surface can also induce the damage to the sp^2 structure of the graphene channel and thus prejudice signal transduction (Niyogi et al., 2010).

Therefore, the AchE was immobilized via electrostatic interactions by employing a solution of higher pH than its PI (5.3) (Leuzinger et al., 1968), at which the protein is negatively charged. The anchoring was observed in the FET response as a shifting in the Dirac point to more positive potentials (Fig. S6), coherent with negatively charged species adsorption; i.e., a p-doping effect (Wang and Burke, 2014). Furthermore, no significant changes in the form of the transfer curve were observed, indicating no deterioration of the gFET. Contrarily, Sohn et al. reported a decrease in the sensor sensitivity of approximately 50% after the

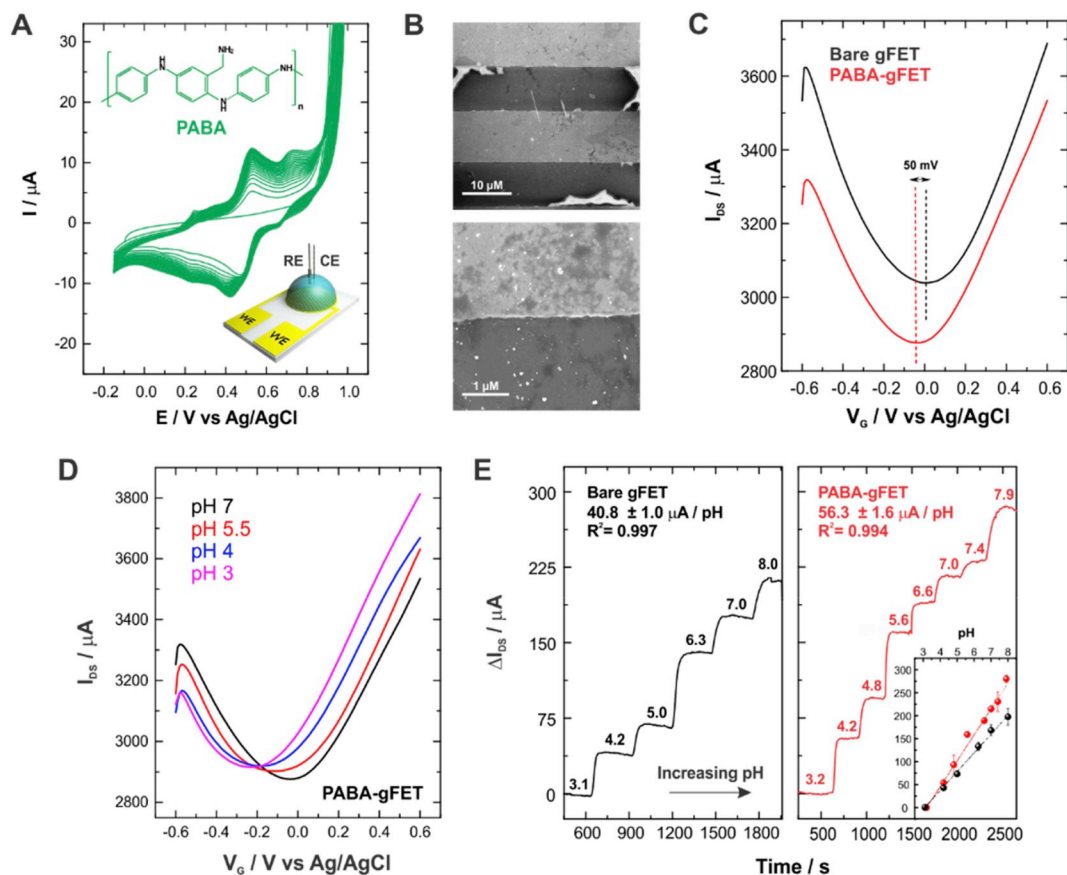


Fig. 2. Voltammograms for the electropolymerization of PABA (H_2SO_4 0.5M, 50 mV/s, 20 cycles) onto a gFET and illustration of the configuration used (A). SEM images of a PABA-gFET (B). Transfer characteristics of the same gFET before and after PABA electrodeposition (KCl 10 mM, HEPES 0.1 mM, pH 7) (C). PABA-gFET transfer characteristics while changing the pH of the electrolyte solution from 3 to 7 in HEPES 0.1 mM and KCl 10 mM buffer (D). pH sensitivity curves at a fixed gate potential ($V_G = -0.2 \text{ V}$, $V_{\text{DS}} = 0.1 \text{ V}$) for the same gFET before (bare) and after PABA electropolymerization (E).

covalent immobilization of AchE on rGO-gFETs (Sohn et al., 2013). Quantification of the amount of immobilized AchE was performed by SPR (see SI), yielding a mass surface coverage of 290 ng cm^{-2} , which agrees with typical AchE surface coverages (Milkani et al., 2011).

2.4. Acetylcholine sensing

Firstly, the signal transduction mechanism of the biosensors was studied by analyzing the static response. The transfer characteristics of an AchE-PABA-gFET in the absence (dashed black line) and presence (solid red line) of $75 \mu\text{M}$ acetylcholine are shown in Fig. 3A. A clear shift of the Dirac point to more negative potentials can be noticed in the presence of the substrate, coherent with a shift obtained upon decreasing the pH of the solution. This outcome reveals that the AchE effectively catalyze the hydrolysis of acetylcholine, yielding choline and acetic acid (Scheme 1); thus, causing a decrease in the local pH. Then, the pH variation modifies the charge density of PABA triggering a negative shift of the Dirac point.

Furthermore, the real-time flow response of the AchE-PABA-modified transistor to increasing Ach concentration can be seen in Fig. 3B. As was shown in Fig. 3A, the decrease on the local pH due to acetylcholine catalyzed hydrolysis shifts the Dirac point of the gFETs to more negative values. This shift causes a decrease in I_{DS} (at a $V_{\text{DS}} > 0$) as the transistors were biased in the hole regime, where $V_G < V_i$. The continuous flow response of the transistors shows that they can be used for the real-time sensing of Ach. Moreover, the electrolyte gating setup allows for the devices to be operated at very low gate voltages ($V_G = -0.2 \text{ V}$), which has been reported as a critical requirement to minimize the disruption of biological samples or any possible

electrochemical reaction (He et al., 2010).

As can be noticed from Fig. 3B, the flow response of the transistors exhibited a logarithmic sensitivity with the Ach concentration. By assuming that the proton concentration is proportional to Ach (Hess et al., 2014), the logarithmic ratio can be comprehended by evoking the linear response of the gFETs to the pH (Section 3.2); that is, the logarithm of proton concentration. A decrease of the drain-source current of approximately $70 \mu\text{A}$ was observed when flowing through the cell an acetylcholine concentration of 1 mM . Above this concentration, the enzyme could be inhibited by the high substrate concentration (the so-called substrate inhibition) (Wilson and Alexander, 1962). The analysis of the modified gFET response in terms of an enzymatic kinetics model is presented in the SI file.

On the other hand, the variation in I_{DS} can be correlated with a change in the local pH of 1.25 pH units using the sensitivity values obtained for the pH response of the sensors, i.e. from 7.4 to 6.15, consistent with other studies of Ach sensing with gFETs (Chae et al., 2018; Sohn et al., 2013). This change in the pH was reported to diminish the activity of AchE by almost 40% (Bergmann et al., 1958). Finally, the obtained response was totally reversible, as the injection of buffer solution after the highest acetylcholine concentration yielded an increase in the drain-source current to almost the initial value ($\Delta I_{\text{DS}} \sim 0$), implying that the transistors could be reused for further measurements.

Many methods have been described for the construction of acetylcholine sensors by the immobilization of AchE onto amino-containing matrices (Vakurov et al., 2004). In the present case, the fabrication of the biosensors was performed by functionalizing the surface of graphene field effect transistors with PABA, a polymer bearing pendant amino groups, to which the enzyme was anchored. However, the use of PEI also

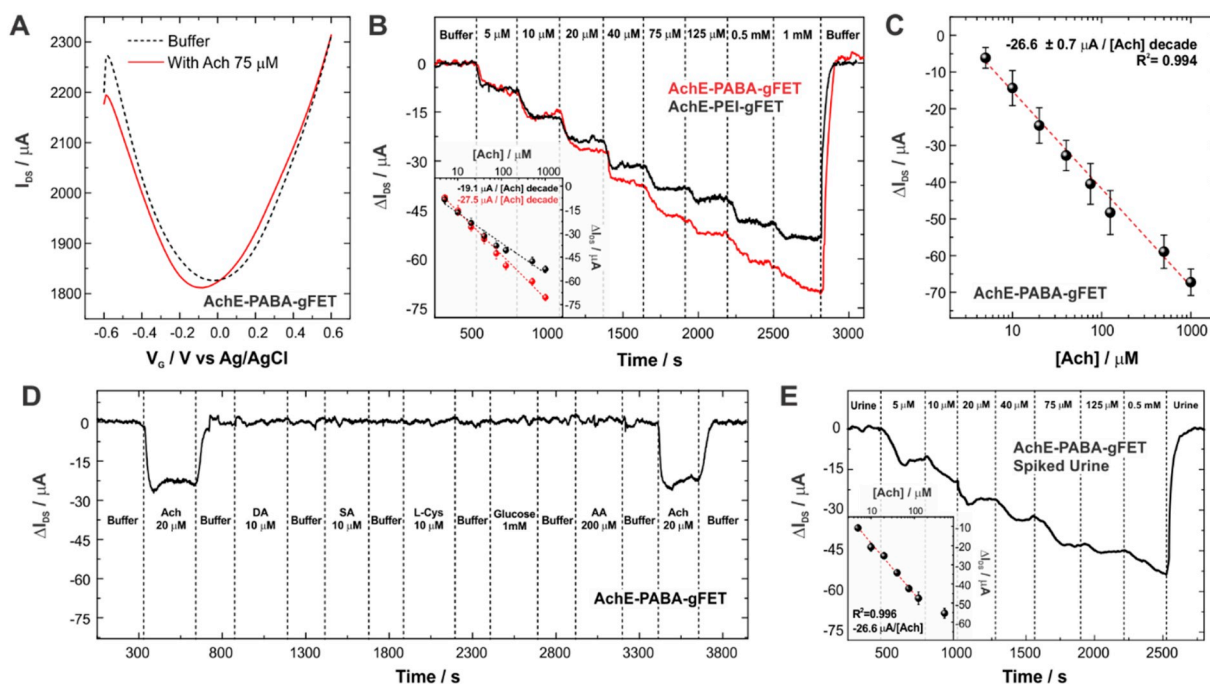


Fig. 3. Transfer characteristics of an AchE-PABA-gFET in the absence and presence of Ach 75 μM ($V_{\text{DS}} = 0.1 \text{ V}$, KCl 10 mM, HEPES 0.1 mM, pH 7) (A). Flow response of an AchE-PABA-gFET and an AchE-PEI-gFET ($300 \mu\text{L min}^{-1}$, $V_{\text{G}} = -0.2 \text{ V}$, $V_{\text{DS}} = 0.1 \text{ V}$) at different acetylcholine concentrations, whereas the inset shows the sensitivity comparison between both systems (two measurements performed) (B). Reproducibility assay for the AchE-PABA-gFETs showing the results obtained for three different electrodes (C). Flow response of an AchE-PABA-gFET ($300 \mu\text{L min}^{-1}$, $V_{\text{G}} = -0.2 \text{ V}$, $V_{\text{DS}} = 0.1 \text{ V}$) while flowing the analyte and different interferences (D). Flow response of an AchE-PABA-gFET ($300 \mu\text{L min}^{-1}$, $V_{\text{G}} = -0.2 \text{ V}$, $V_{\text{DS}} = 0.1 \text{ V}$) while flowing spiked urine samples, whereas the inset shows the linear fitting of the response in a logarithmic scale (two measurements performed). (E).

appears as a promising strategy to build sensing devices, as its assembly onto the channel of rGO transistors has been recently reported to improve the pH sensing parameters of bare gFETs and, concomitantly, it provides anchoring sites for electrostatic enzyme immobilization (Piccinini et al., 2017). In order to compare the performance of the PABA-gFETs with PEI-gFETs for the construction of real-time biosensors, the immobilization of AchE was assessed on both PABA and PEI-SPS-modified gFETs and, subsequently, their response to acetylcholine was studied. It is worth adding that the PEI-gFETs were first modified with SPS in order to confer negative charges to the channel surface and afterwards a layer of PEI was anchored on top by electrostatic interactions. Note that due to the electrochemical procedure of modification, no pyrene anchoring layer was required, constituting an advantage of this functionalization approach.

Results for the AchE-PEI-gFETs system are also presented in Fig. 3B. From the comparison between the PEI and the PABA-functionalized systems, it can be noticed that the sensitivity of AchE-PABA-gFETs ($-27.5 \pm 0.8 \mu\text{A/Ach decade}$, $R^2 = 0.994$) is higher than the one of AchE-PEI-gFETs ($-19.1 \pm 1.1 \mu\text{A/Ach decade}$, $R^2 = 0.975$) (two measurements performed), showing a 43.9% improvement. Moreover, the enhancement on the performance of the biosensors occurs particularly when higher Ach concentrations are injected, meaning lower local pH. This result supports the hypothesis that attributes the higher sensitivity of PABA-gFETs to the multiple protonation states available in PABA. As different amine moieties from both aniline and amino-benzylamine are present in the polymer, different pK_a -values are found in a broader pH range. Secondary amines present in PABA become deprotonated at more acidic pH values than primary ones, improving the pH response in a more acidic medium.

On the other hand, it has been reported that biomolecules in solution can be adsorbed onto the graphene surface, triggering changes in the conductivity or in the charge carrier mobilities (He et al., 2010; Piccinini et al., 2017). Moreover, due to the high sensitivity of the transistors to pH, even very small variations in the pH of the solution can also generate

changes on the current recorded. Considering these factors, the non-specific response of the polymer-modified transistors to different neurotransmitter solutions was examined preceding the enzyme immobilization onto the polymer layer. Real-time measurements increasing the neurotransmitter concentration from 10 μM to 1 mM were performed on PABA-gFETs (Fig. S7) and no significant changes on I_{DS} were observed while flowing different concentrations of acetylcholine.

Different figures of merit of the AchE-PABA-gFETs as repeatability, reproducibility and stability were also studied (Justino et al., 2010). The relative standard deviation (RSD) for repeatability was 4.9% for four successive measurements of 75 μM urea. The biosensors reproducibility was investigated by preparing three different AchE-PABA-gFETs and monitoring the real-time Ach flow response in the range of 5–1000 μM (Fig. 3C). The transistors sensitivities exhibited a very low RSD of 2.6%, revealing excellent device-to-device reproducibility. Moreover, the biosensors showed a fast response time, with an average value of 130 s for 95% of the maximum response. The stability of the devices was also studied, and it was found that, by storing the electrodes at 4 $^{\circ}\text{C}$ in buffer HEPES solution, they retained almost 94% of the original response after 4 days of storage. The limit of detection (LOD) of our biosensor was calculated as 3 times the standard deviation for the buffer injection (blank), yielding a value of 2.3 μM .

The selectivity of the biosensors relative to a variety of potential interferences known to be present in the extracellular milieu was also tested (Fig. 3D and Fig. S8). Glucose, ascorbic acid (AA) and neurotransmitters dopamine (DA) and serotonin (SA), as well as other endogenous electroactive species as L-cysteine (L-Cys), were injected after 20 μM Ach flow detection and buffer washing. The concentrations of potential interferences tested were at levels that occur in brain ECF (Mitchell, 2004); the electroactive neurotransmitters DA and SA are typically present at concentrations much lower than 10 μM and therefore should have little effect on sensor response. The endogenous electroactive species, as AA, are usually those that present the greatest potential interference. The typical ECF concentrations of AA fluctuate in

the range 100–300 μM (Mitchell, 2004). The transistors did not show significant I_{DS} changes in the presence of the interferences and the response to Ach was recovered by 97.5% after the whole set of interferences injected.

Moreover, in order to study the response of the biosensor in a real biological fluid, we performed flow measurements of Ach spiked diluted urine samples (1:5) (Fig. 3E). The device showed similar sensitivity to that reported in the buffer solution, proving that it can be used to sense the neurotransmitter in more complex matrices. Note, however, that in the case of using concentrated buffer solutions the sensitivity of the device could be affected due to the concomitant effect of the bulk buffer capacity on the local proton concentration.

Finally, Table S1 shows a comparison of major analytical figures of merit between the present biosensor and other recently reported enzymatic FETs for Ach detection. Transistors presented in this work show remarkable features, such as high sensitivity, wide detection range and low detection limit, while being operated at small applied potentials (V_{G} and V_{DS}). Particularly when compared with similar devices involving the immobilization of AchE on graphene FETs, this device merges the above-mentioned features with the possibility of performing measurements in continuous flow conditions, making feasible the real-time sensing of the neurotransmitter.

3. Conclusions

We presented a new strategy for the rational construction of gFET-based systems using electropolymerization as integration approach. The voltammetric synthesis of PABA, an electroactive polymer film with pendant amine moieties, allowed the immobilization of functional AchE and, simultaneously, the enhancement of the pH response of gFETs. The higher sensitivity to pH changes was ascribed to the wide pKa distribution of PABA caused by a variety of amine/imine groups.

The AchE-PABA-gFETs showed a shift in the Dirac point to more negative values in the presence of acetylcholine due to enzyme-catalyzed hydrolysis, allowing for the real-time sensing of the neurotransmitter in the range 5–1000 μM . Moreover, AchE-PABA-gFETs showed excellent selectivity to interferences, fast response time and good reproducibility. The sensors were even checked in real urine samples, with a similar sensitivity to that observed in buffer. Compared with similar reported gFET sensors, the AchE-PABA-gFETs present better response in flow conditions and a lower LOD.

Finally, the proposed strategy represents a promissory method for the construction of biosensors due to the advantages of the voltammetric electro-synthesis, such as precise control of the film thickness, stability and no necessity of chemical primers. On the other hand, the electro-synthesized polyelectrolyte constitutes a scarcely explored electroactive polymer with many proved advantages as building block compared to the wide-employed Pani, particularly when dealing with soft acidic or neutral media, as those needed for most enzymes to work. Thus, the functionalization approach could be extended to the integration of other enzymes or even nanomaterials, which could expand the sensing applications.

Declaration of competing interest

The authors declare that they have no known competing financial interests or personal relationships that could have appeared to influence the work reported in this paper.

CRediT authorship contribution statement

Gonzalo E. Fenoy: Conceptualization, Formal analysis, Investigation, Methodology, Writing - original draft. **Waldemar A. Marmisollé:** Conceptualization, Formal analysis, Investigation, Methodology, Writing - original draft. **Omar Azzaroni:** Conceptualization, Formal analysis, Investigation, Methodology, Writing - review & editing.

Wolfgang Knoll: Conceptualization, Formal analysis, Investigation, Methodology, Writing - review & editing.

Acknowledgments

Financial support from ANPCyT (PICT 2015–0239, 2016–1680, 2017–1523), CEST–UNLP Partner Lab for Bioelectronics and UNLP (PPID-X016) is greatly acknowledged. SEM measurements by Patrik Aspermaier and SPR measurements by Dr. Sebastián Alberti are gratefully acknowledged. W.A.M., and O.A. are CONICET staff members. G.E.F. acknowledges CONICET for a doctoral fellowship and thanks the Biosensors Technologies Group for support provided during his stay at AIT.

Appendix A. Supplementary data

Supplementary data to this article can be found online at <https://doi.org/10.1016/j.bios.2019.111796>.

References

- Andrescu, S., Marty, J.L., 2006. Twenty years research in cholinesterase biosensors: from basic research to practical applications. *Biomol. Eng.* 23, 1–15. <https://doi.org/10.1016/j.bioeng.2006.01.001>.
- Androneanu, C., Schuhmann, W., 2017. Graphene-based field effect transistors as biosensors. *Curr. Opin. Electrochem.* 3, 11–17. <https://doi.org/10.1016/j.coelec.2017.03.002>.
- Bergmann, F., Rimon, S., Segal, R., 1958. Effect of pH on the activity of eel esterase towards different substrates. *Biochem. J.* 68, 493–499. <https://doi.org/10.1042/bj0680493>.
- Berninger, T., Bliem, C., Piccinini, E., Azzaroni, O., Knoll, W., 2018. Cascading reaction of arginase and urease on a graphene-based FET for ultrasensitive, real-time detection of arginine. *Biosens. Bioelectron.* 115, 104–110. <https://doi.org/10.1016/j.bios.2018.05.027>.
- Bliem, C., Piccinini, E., Knoll, W., Azzaroni, O., 2018. Enzyme multilayers on graphene-based FETs for biosensing applications. *Methods Enzymol.* 609, 23–46. <https://doi.org/10.1016/bs.mie.2018.06.001>.
- Chae, M.S., Yoo, Y.K., Kim, J., Kim, T.G., Hwang, K.S., 2018. Graphene-based enzyme-modified field-effect transistor biosensor for monitoring drug effects in Alzheimer's disease treatment. *Sens. Actuators B Chem.* 272, 448–458. <https://doi.org/10.1016/j.snb.2018.06.010>.
- Chakrabarti, M.H., Low, C.T.J., Brandon, N.P., Yufit, V., Hashim, M.A., Irfan, M.F., Akhtar, J., Ruiz-Trejo, E., Hussain, M.A., 2013. Progress in the electrochemical modification of graphene-based materials and their applications. *Electrochim. Acta* 107, 425–440. <https://doi.org/10.1016/j.electacta.2013.06.030>.
- Diao, J., Yu, X., Ma, L., Li, Y., Sun, Y., 2018. Protein surface structural recognition in inactive areas: a new immobilization strategy for acetylcholinesterase. *Bioconjug. Chem.* 29, 1703–1713. <https://doi.org/10.1021/acs.bioconjugchem.8b00160>.
- Fenoy, G.E., Giussi, J.M., von Bilderling, C., Maza, E.M., Pietrasanta, L.L., Knoll, W., Marmisollé, W.A., Azzaroni, O., 2018. Reversible modulation of the redox activity in conducting polymer nanofilms induced by hydrophobic collapse of a surface-grafted polyelectrolyte. *J. Colloid Interface Sci.* 518, 92–101. <https://doi.org/10.1016/j.jcis.2018.02.014>.
- Fenoy, Gonzalo E., Scotto, J., Azcárate, J., Rafti, M., Marmisollé, W.A., Azzaroni, O., 2018. Powering up the oxygen reduction reaction through the integration of O₂-adsorbing metal-organic frameworks on nanocomposite electrodes. *ACS Appl. Energy Mater.* 1, 5428–5436. <https://doi.org/10.1021/acsaem.8b01021>.
- Fu, W., Jiang, L., van Geest, E.P., Lima, L.M.C., Schneider, G.F., 2017. Sensing at the surface of graphene field-effect transistors. *Adv. Mater.* 29, 1603610. <https://doi.org/10.1002/adma.201603610>.
- He, Q., Sudibya, H.G., Yin, Z., Wu, S., Li, H., Boey, F., Huang, W., Chen, P., Zhang, H., 2010. Micropatterns of reduced graphene oxide films: fabrication and sensing applications. *Am. Chem. Soc. Nano* 4, 3201–3208. <https://doi.org/10.1021/nn100780v>.
- Hess, L.H., Lyuleeva, A., Blaschke, B.M., Sachsenhauser, M., Seifert, M., Garrido, J.A., Deubel, F., 2014. Graphene transistors with multifunctional polymer brushes for biosensing applications. *ACS Appl. Mater. Interfaces* 6, 9705–9710. <https://doi.org/10.1021/am502112x>.
- Justino, C.L.L., Rocha-Santos, T.A., Duarte, A.C., 2010. Review of analytical figures of merit of sensors and biosensors in clinical applications. *TrAC Trends Anal. Chem.* (Reference Ed.) 29, 1172–1183. <https://doi.org/10.1016/j.trac.2010.07.008>.
- Kergoat, L., Piro, B., Simon, D.T., Pham, M.C., Noël, V., Berggren, M., 2014. Detection of glutamate and acetylcholine with organic electrochemical transistors based on conducting polymer/platinum nanoparticle composites. *Adv. Mater.* 26, 5658–5664. <https://doi.org/10.1002/adma.201401608>.
- Kong, D., Jin, R., Zhao, X., Li, H., Yan, X., Liu, F., Sun, P., Gao, Y., Liang, X., Lin, Y., Lu, G., 2019. Protein-inorganic hybrid nanoflower-rooted agarose hydrogel platform for point-of-care detection of acetylcholine. *ACS Appl. Mater. Interfaces* 11, 11857–11864. <https://doi.org/10.1021/acsaami.8b21571>.
- Kotlowski, C., Aspermaier, P., Khan, H.U., Reiner-Rozman, C., Breu, J., Szunerits, S., Kim, J.J., Bao, Z., Kleber, C., Pelosi, P., Knoll, W., 2018. Electronic biosensing with

- flexible organic transistor devices. *Flex. Print. Electron.* 3, 34003. <https://doi.org/10.1088/2058-8585/aad433>.
- Leuzinger, W., Baker, A.L., Cauvin, E., 1968. Acetylcholinesterase. II. Crystallization, absorption spectra, isoionic point. *Proc. Natl. Acad. Sci. U. S. A* 59, 620–623. <https://doi.org/10.1590/1678-7757-2016-0408>.
- Marmisollé, W.A., Florit, M.I., Posadas, D., 2014. Acid-base equilibrium in conducting polymers. The case of reduced polyaniline. *J. Electroanal. Chem.* 734, 10–17. <https://doi.org/10.1016/j.jelechem.2014.03.003>.
- Marmisollé, W.A., Gregurec, D., Moya, S., Azzaroni, O., 2015. Polyanilines with pendant amino groups as electrochemically active copolymers at neutral pH. *ChemElectroChem* 2, 2011–2019. <https://doi.org/10.1002/celc.201500315>.
- Milkani, E., Lambert, C.R., McGimpsey, W.G., 2011. Direct detection of acetylcholinesterase inhibitor binding with an enzyme-based surface plasmon resonance sensor. *Anal. Biochem.* 408, 212–219. <https://doi.org/10.1016/j.ab.2010.09.009>.
- Mitchell, K.M., 2004. Acetylcholine and choline amperometric enzyme sensors characterized in vitro and in vivo. *Anal. Chem.* 76, 1098–1106. <https://doi.org/10.1021/ac034757v>.
- Niyogi, S., Bekyarova, E., Itkis, M.E., Zhang, H., Shepperd, K., Hicks, J., Sprinkle, M., Berger, C., Lau, C.N., Deheer, W.A., Conrad, E.H., Haddon, R.C., 2010. Spectroscopy of covalently functionalized graphene. *Nano Lett.* 10, 4061–4066. <https://doi.org/10.1021/nl1021128>.
- Piccini, E., Bliem, C., Reiner-Rozman, C., Battaglini, F., Azzaroni, O., Knoll, W., 2017. Enzyme-polyelectrolyte multilayer assemblies on reduced graphene oxide field-effect transistors for biosensing applications. *Biosens. Bioelectron.* 92, 661–667. <https://doi.org/10.1016/j.bios.2016.10.035>.
- Raffa, D.L., Leung, K.T., Battaglini, F., 2006. Electrochemical copolymerization of aniline and ortho-aminobenzylamine. Studies on its conductivity and chemical derivatization. *J. Electroanal. Chem.* 587, 60–66. <https://doi.org/10.1016/j.jelechem.2005.10.017>.
- Ray, A., Richter, A.F., MacDiarmid, A.G., Epstein, A.J., 1989. Polyaniline: protonation/deprotonation of amine and imine sites. *Synth. Met.* 29, 151–156. [https://doi.org/10.1016/0379-6779\(89\)90290-7](https://doi.org/10.1016/0379-6779(89)90290-7).
- Reiner-Rozman, C., Schodl, J., Nowak, C., Kleber, C., 2015. Scanning electrochemical microscopy as a characterization tool for reduced graphene oxide field effect transistors. *e-J. Surf. Sci. Nanotechnol.* 13, 366–372. <https://doi.org/10.1380/ejsnt.2015.366>.
- Salvo, P., Melai, B., Calisi, N., Paoletti, C., Bellagambi, F., Kirchhain, A., Trivella, M.G., Fuoco, R., Di Francesco, F., 2018. Graphene-based devices for measuring pH. *Sens. Actuators B Chem.* 256, 976–991. <https://doi.org/10.1016/j.snb.2017.10.037>.
- Sangubotla, R., Kim, J., 2018. Recent trends in analytical approaches for detecting neurotransmitters in Alzheimer's disease. *TrAC Trends Anal. Chem. (Reference Ed.)* 105, 240–250. <https://doi.org/10.1016/j.trac.2018.05.014>.
- Sattarahmady, N., Heli, H., Moosavi-Movahedi, A.A., 2010. An electrochemical acetylcholine biosensor based on nanoshells of hollow nickel microspheres-carbon microparticles-Nafion nanocomposite. *Biosens. Bioelectron.* 25, 2329–2335. <https://doi.org/10.1016/j.bios.2010.03.031>.
- Sheldon, R.A., van Pelt, S., 2013. Enzyme immobilisation in biocatalysis: why, what and how. *Chem. Soc. Rev.* 42, 6223–6235. <https://doi.org/10.1039/c3cs60075k>.
- Sohn, I.Y., Kim, D.J., Jung, J.H., Yoon, O.J., Nguyen Thanh, T., Tran Quang, T., Lee, N.E., 2013. PH sensing characteristics and biosensing application of solution-gated reduced graphene oxide field-effect transistors. *Biosens. Bioelectron.* 45, 70–76. <https://doi.org/10.1016/j.bios.2013.01.051>.
- Vakurov, A., Simpson, C.E., Daly, C.L., Gibson, T.D., Millner, P.A., 2005. Acetylcholinesterase-based biosensor electrodes for organophosphate pesticide detection. *Biosens. Bioelectron.* 20, 2324–2329. <https://doi.org/10.1016/j.bios.2004.07.022>.
- Vakurov, A., Simpson, C.E., Daly, C.L., Gibson, T.D., Millner, P.A., 2004. Acetylcholinesterase-based biosensor electrodes for organophosphate pesticide detection: I. Modification of carbon surface for immobilization of acetylcholinesterase. *Biosens. Bioelectron.* 20, 1118–1125. <https://doi.org/10.1016/j.bios.2004.03.039>.
- Wang, Y.Y., Burke, P.J., 2014. Polyelectrolyte multilayer electrostatic gating of graphene field-effect transistors. *Nano Res.* 7, 1650–1658. <https://doi.org/10.1007/s12274-014-0525-9>.
- Wilson, I.B., Alexander, J., 1962. Acetylcholinesterase: reversible inhibitors, substrate inhibition. *J. Biol. Chem.* 237, 1323–1327.
- World Health Organization, 2006. *Neurological Disorders: Public Health Challenges*. World Heal. pp. 86–87. The Organ.
- Zhang, M., Liao, C., Mak, C.H., You, P., Mak, C.L., Yan, F., 2015. Highly sensitive glucose sensors based on enzyme-modified whole-graphene solution-gated transistors. *Sci. Rep.* 5, 1–6. <https://doi.org/10.1038/srep08311>.
- Zuccaro, L., Krieg, J., Desideri, A., Kern, K., Balasubramanian, K., 2015. Tuning the isoelectric point of graphene by electrochemical functionalization. *Sci. Rep.* 5, 11794. <https://doi.org/10.1038/srep11794>.